Green Chemistry

Paper

Novel biomass-derived aldehyde tanning agents with in-situ dyeing properties: a 'Two Birds with One Stone' strategy for engineering chrome-free and dye-free colored leather

Received 00th January 20xx,
Accepted 00th January 20xx

DOI: 10.1039/x0xx00000x

Wei Ding [a,b*], Javier Remón [c], Zhicheng Jiang [d*]

High-profile chrome (Cr) pollution from tanning and potential health hazards from released leather dyes and pigments in leather products restrict the sustainable development of the leather industry. Herein, we report on a novel 'Two Birds with One Stone' strategy to simultaneously eliminate Cr and colorant pollutions using a Cr-free tanning agent with in-situ dyeing ability. Sucralose, containing an electron-withdrawing group (−Cl), was employed to fabricate a biomass-derived aldehyde tanning agent with in-situ dyeing properties (BAT-iDP). This agent formed Schiff-base crosslinks between its aldehyde groups and the amino groups of collagen fibers (CFs), which efficiently dispersed and fixed the CFs, producing a tanned leather with sufficient thermal stability (80.2 °C of shrinkage temperature) to meet commercial requirements. Simultaneously, the presence of an auxochrome (−Cl) in the structure of the Schiff-bases formed endowed the tanned leather with a brown color characteristic of leather. As a result, the tanned leather produced with our 'Two Birds with One Stone' strategy had excellent dyeing uniformity, color fastness to dry-wet rubbing and favorable mechanical strengths (14.7 N/mm^2 of tensile strength and 46.3 N/mm of tear strength). This novel approach provides new insights for designing and developing multifunctional sustainable materials towards a greener and carbon-neutral leather industry.

Introduction

The leather industry is one of the essential pillars of the light industry manufacturing goods for people's daily life. Raw materials of leather are green, natural, and readily available, and the products produced from leather are commonly and worldwide used. However, in recent years, impacted by the environmental pollution issues from leather making, the global leather industry is facing severe challenges, among which chrome pollution is a key bottleneck restricting the ecological development of the leather industry. [1–3] Currently, chrome tanning is still the most widely used tannage as it can endow leather with excellent thermal stability and organoleptic properties via forming robust coordination crosslinking structures in the leather matrix. In fact, in addition to the coordination crosslinking formed via metal tanning, covalent crosslinking formed via organic tanning can also endow leather with stable tanning properties. From the perspective of eliminating chrome pollution, the development and application of organic tanning agents with a 'metal-free' feature is a vital strategy to break through the Cr-related pollution bottleneck for the greenization of the leather industry. [4]

Among the existing organic tanning agents, aldehyde-based tanning materials, including oxazolidine, [5] modified glutaraldehyde, [6] organic phosphonium salts, [7] and commercial amphoteric organic tanning agents [8,9] have good and stable tanning properties. These are attributed to their high activity to bond with the $-NH_2$ in the collagen fibers (CFs) via constructing a robust covalent crosslinking structure. However, the continuous formaldehyde (FA) release from these tanned leathers during commercial use is difficult to avoid, [10,11] resulting in excessive FA in the leather products. Besides, the aldehyde organic tanning agents mentioned above result in the tanned leather with a low isoelectric point, causing poor absorption and fixation of the commonly used wet-finishing materials. [12] As a higher hazard potential due to the presence of dyeing species in the wastewater, making the wastewater treatment more challenging. [13] Too low dye-fixation degree and color-fastness may also cause the discolor of the leather products during use, [14] thus lowering their quality grade. More importantly, the severe migration of hazardous synthetic leather dyes will cause potential hazards to human health. [15,16]

Given these potential hazards, constructing an integrated processing system with high safety for organic tanning with high dyeing efficiency is critical to developing chrome-free tanning technologies. This could help achieve a more ecological and sustainable leather industry in the medium term. For this, Liu et al. prepared amphoteric wet finishing materials to improve the dye uptake in the post-tanning of organic-tanned leather. [9] Ding et al. synthesized a polymeric dye for the high-performance dyeing of biomass-derived aldehyde tanned leather. [14] Despite achieving high dyeing efficiency via these strategies, some hazardous synthetic dyes remain in the wastewater. Given this, designing new and stable

[a] China Leather and Footwear Research Institute Co. Ltd., Beijing 100015, P. R. China. E-mail: dingwei1368@outlook.com
[b] Key Laboratory of Leather and Footwear Green Manufacturing Technology of China Light Industry, Beijing 100015, P. R. China.
[c] Instituto de Carboquímica, CSIC, Zaragoza, 50018, Spain.
[d] National Engineering Research Center of Clean Technology in Leather Industry, Sichuan University, Chengdu, 610065, P. R. China. E-mail: zhichengjiang@scu.edu.cn

Electronic Supplementary Information (ESI) available: [details of any supplementary information available should be included here]. See DOI: 10.1039/x0xx00000x

organic tanning agents with satisfactory tanning effects and in-situ dyeing properties is an attractive strategy that can simultaneously solve chrome pollution, formaldehyde release and poor absorption-fixation of dye. At present, leather materials with tanning and coloring functions have been explored. These include reactive dyes with aldehyde groups, [17] natural iridoid compounds [18–20] and vegetable tannin extracts [21]. However, these chemicals do not simultaneously have good tanning and dyeing properties when used as tanning agents.

As a sort of renewable and non-toxic bioresource, saccharide-based biomass (SBM) containing vicinal diol structures can be selectively oxidized into a biodegradable product, which can be used as a kind of biomass-derived aldehyde tanning agent (BAT). [22,23] As shown in Fig. 1a, BAT can react with the -NH_2 on skin CFs under an alkali tanning condition to form intra- and intermolecular Schiff-base crosslinks, [23] thereby exhibiting stable tanning capability. [24–26] However, the single structure of conventional SBM with only C, H, and O endows the BAT tanned leather with pale color. Thus, additional dyeing of this leather is highly needed to meet the standard color requirements for commercial use. On the contrary, a *β*-elimination reaction may generate a C=C structure under alkaline tanning conditions (Fig. 1b), [27,28] along with another a conjugated structure that can absorb specific visible light [29,30] and can probably help manufacture a tanning agent with good tanning and dyeing features.

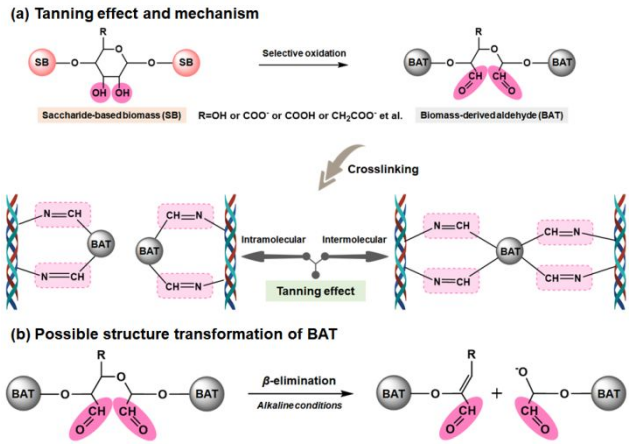

Fig. 1. Illustration of the tanning mechanism of BAT (a) and the possible structure transformation of BAT under alkaline tanning conditions (b).

Inspired by this, this work presents novel engineering solutions to develop organic tanning agents with simultaneous good tanning and in-situ dyeing properties, i.e., a 'Two Birds with One Stone' strategy. For this, biomass-derived sucralose containing specific auxochromes (−Cl) has been used to prepare a BAT with in-situ dyeing properties (BAT-iDP). The structural features of our BAT-iDP were characterized by FTIR and NMR analyses, and its tanning effects and in-situ dyeing performances were systematically investigated on some physical leather properties, such as thermal stability, fiber dispersion and color-fastness. The dyeing performances and physical properties of BAT-iDP crust leather were compared with those of conventional BAT crust leather colored by small dye (SD) and conventional dye (CD). Therefore, our novel "Two Birds with One Stone" strategy represents a landmark achievement towards developing bi-functional and eco-friendly organic tanning agents, which can pave the wave to replace hazardous tanning agents and dyeing pigments with more environmentally benign alternatives. This work can also provide new insights for the development of novel green materials and leather processing technology systems.

Results and discussion

Structural features of BAT-iDP

Sucralose was firstly oxidized to BAT-iDP in a $NaIO_4$ solution at 10 ºC for 12 h, and the obtained product was characterized by FTIR and NMR analyses. As illustrated in Fig. 2b, the peak at 3390 cm^{-1} in the FTIR spectrum of sucralose shifts to 3471 cm^{-1} for BAT-iDP and becomes broader after being oxidized by periodate. Importantly, in the FTIR spectrum of BAT-iDP, a new peak assigned to the aldehyde group (−CH=O) appears at 1733 cm^{-1}. [31] Besides, both the ^{1}H NMR signal at 8.17 ppm, assigning to the protons of −CH=O (Fig. 2c), [32] and the ^{13}C NMR signal at 171.9 ppm, assigning to the carbonyl carbon (C=O) (Fig. 2d), [33] demonstrate the generation of −CH=O after oxidation. Of note, a strong narrow-peak, similar to that of sucralose at 638 cm^{-1}, appears at 616 cm^{-1}, thus indicating the reservation of the electron-withdrawing group (−Cl). According to these data, the successfully prepared BAT-iDP contains −CH=O and an electron-withdrawing group (−Cl). Therefore, it possesses the covalent crosslinking capability for pickled hide along with a conjugated structure with auxochrome (−Cl) species to exhibit in-situ dyeing properties.

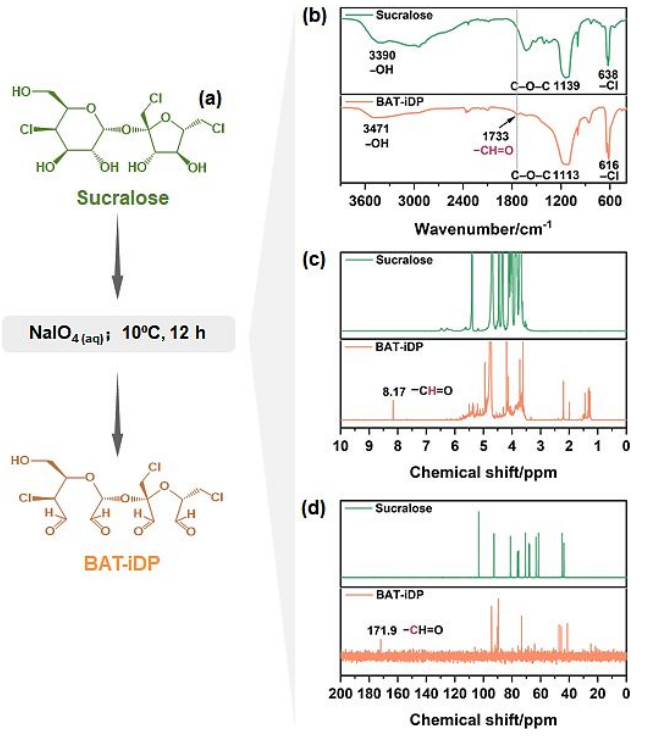

Fig. 2. Structure diagram (a), FTIR (b), and NMR (c, d) spectra of sucralose and BAT-iDP.

Tanning-dyeing performances of BAT-iDP

The BAT-iDP was further used for tanning the pickled cattle hide to clarify its tanning and dyeing performances. After tanning, the dispersion of collagen fibers (CFs) was observed by analyzing the cross-section of the tanned leather using SEM (Fig. 3a). The results show well-dispersed CFs due to the crosslinking between the BAT-iDP and CFs. Then, the shrinkage temperature (Ts) was employed to evaluate the tanning effect of the BAT-iDP (Fig. 3b). Tanned leather with a much higher Ts (80.2 °C) than that of the pickled hide (62.3 °C) is obtained using our new BAT-iDP, which confirms the favorable tanning effect of this agent. Generally, a higher thermal stability of leather means a more robust crosslinking network, [34,35] this property of the pickled hide and BAT-iDP tanned leather was further investigated through thermogravimetric analysis (Fig. 3c and d). The comparison between the thermal stability of both materials reveals an increase in the decomposition temperature. For example, the temperature required for the thermal decomposition of 5 wt.% of the material ($T_{5\%}$) is 97.3 °C for the pickled hide. For the BAT-iDP tanned leather, this is 113.7 °C. Furthermore, in the range of normal temperature to 120 °C, the maximum weight loss peak temperature is 74.3 °C for the pickled hide, while this shifts to 91.4 °C for the BAT-iDP tanned leather, probably owing to the loss of absorbed and bounded water in the CFs matrix. [36] Besides, the primary decomposition temperature of the pickled hide (313.3 °C) is lower in comparison with that of the BAT-iDP tanned leather (318.2 °C). The aforementioned results demonstrate that the as-prepared BAT-iDP has a favorable tanning effect of fixing the CFs in leather via forming stable crosslinking networks, consequently improving the thermal stability of the tanned leather.

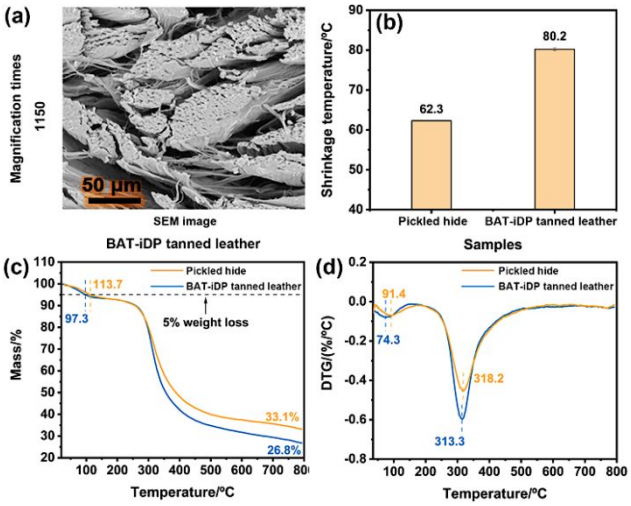

Fig. 3. Tanning effects of BAT-iDP on cattle hide.

Fig. 4a shows differences in the color of the collagen matrix between the pickled cattle hide and the tanned leather. As expected, the tanned leather was in-situ dyed by the BAT-iDP and has a reddish-brown color in the wet state, while the color of BAT tanned leather was still off-white. Such a difference demonstrates the dying capabilities of the BAT-iDP in comparison to those of the BAT. Consequently, after post-tanning, the BAT-iDP tanned leather did not require specialized dyeing to become a light brown crust leather. On the contrary, the BAT tanned leather should undergo additional dyeing to be colored crust leather. To gain more insights into the difference between the original BAT and the improved BAT-iDP, the in-situ dyeing performance of crust leather tanned by BAT-iDP (BAT-iDP crust leather) was further evaluated. For this, a comparison between the dyeing performance of the BAT-iDP was compared to those obtained with the BAT and subsequently dyed with SD and CD (defined as SD-BAT crust leather and CD-BAT crust leather). Overall, the BAT-iDP crust leather color is close to that of the CD-BAT crust leather, which is quite distinct from that of the SD-BAT crust leather. In detail, the dyeing uniformity and dry-wet rubbing resistance of these three pieces of crust leather were characterized and compared. As shown in Fig. 4b, the color uniformity of the three kinds of crust leathers was evaluated by the STDEV value of ΔE, in which the lower this value, the smaller is the color difference among the regions on the crust leather, which translates in high dyeing uniformity. These calculations show that the BAT-iDP crust leather and the CD-BAT crust leather have comparable dyeing uniformity that is superior to that of the SD-BAT crust leather, indicating the desirable covering power of the BAT-iDP, which also allows an in-situ chromogenic structure to be formed. Furthermore, the BAT-iDP crust leather performs best on dry-rubbing and wet-rubbing resistances, while neither CD-BAT nor SD-BAT crust leathers possess these two capabilities (Fig. 4c and d).

To verify the coloring fastness of the BAT-iDP, the aqueous extracts from different crust leathers were determined by UV analysis. The extract liquor from the BAT-iDP crust leather has no absorption in the visible light region, and its color is highly comparable to that of UPW (ultrapure water) (Fig. 4e), indicating the high binding strength of the coloring components inherited from the BAT-iDP. In comparison, orange or light-yellow color is observed for the extract liquors from SD-BAT and CD-BAT crust leathers with remarkable absorptions in the visible light region (Fig. 4f and g). This suggests that lots of colorants were extracted from the crust leather and that the binding strength was weak. This demonstrated that BAT-iDP exhibited favorable coloring fastness, with this being significantly quicker than that of SD and CD. The main reason for this difference may be the differentiated combination ways of the chromophores in the tanned leather. The above results successfully verified our initial hypothesis, i.e., utilizing SBM containing specific auxochromes to prepare sustainable tanning agents with dual properties of tanning and dyeing, (BAT-iDP) has the potential to synergistically address the chrome pollution from tanning and the potential health hazards from released leather dyes in leather products.

Green Chemistry

ARTICLE

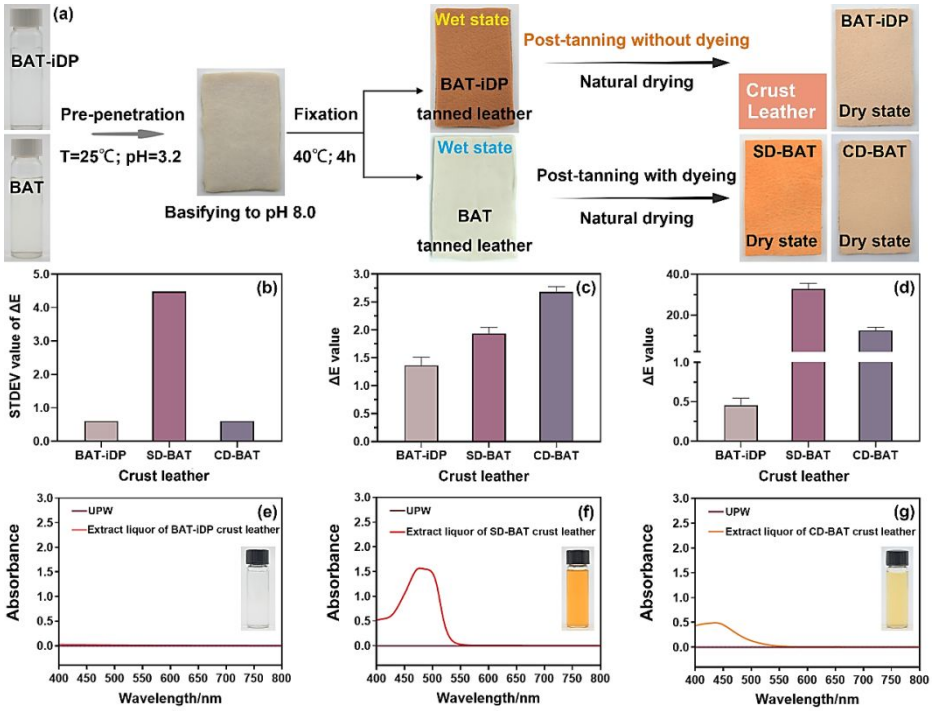

Fig. 4. Color change of leather during tanning and post-tanning (a), coloring uniformity (b), coloring fastness (c: dry-rubbing resistance; d: wet-rubbing resistance) of crust leather, and the visible spectra of crust leather extract liquors (e: BAT-iDP; f: SD-BAT; g: CD-BAT).

Tanning and in-situ dyeing mechanism of BAT-iDP

Based on the tanning theory, it is the sidechains of collagen that largely define its reactivity and its ability to be modified by the stabilizing reactions of tanning, when leather is made. For aldehyde tanning, Lys is one of the most important and typical amino acids that provide the collagen fiber with sidechains containing free amino groups to react with aldehydes, which is highly responsible for the aldehydic tanning effect. [10] Thus, Lys is commonly used as a model compound of collagen to investigate the interactions between aldehydes and collagen fibers. [37] Accordingly, to understand the tanning and in-situ dyeing mechanism of the BAT-iDP, its reaction with Lys was studied under an alkaline medium (pH=8.0) at 40 °C for 4 h. Then, BAT-iDP, Lys, and their reaction product (MP) were analyzed by FTIR, NMR, and UV-vis spectra (Fig. 5). The FTIR of MP inherited the spectra of BAT-iDP and Lys, which shows peaks at 1627 cm^{-1} (−C=N, characteristic of imine) and 1368 cm^{-1} ($-COO^-$ symmetric stretching). [38] The absorption peak at 1733 cm^{-1} assigned to the C=O stretching disappears in the spectrum of MP compared with BAT-iDP. This absent absorption band and the absorption peaks at 1627 cm^{-1} demonstrated that the Schiff-base (C=N) formed between the −CH=O of BAT-iDP and the $-NH_2$ of Lys. [39] It should be noted that the C-6 resonance of Lys (39.4 ppm) moves toward higher fields (39.1 ppm) in the MP, which may be caused by the combination between Lys and BAT-iDP. [39] More importantly, the resonance peak of the Schiff-base at 160.5 ppm (C-b) is observed, [40,41] suggesting the successful reaction between the BAT-iDP and Lys.

Fig. 5e shows the UV-vis spectra of BAT, BAT-iDP, Lys, the reaction product between BAT-iDP and Lys (MP), and between BAT-iDP and Lys (BLP). These data reveal that the BAT-iDP has a meager absorption in the visible region while Lys has significant absorption in the visible region. The absorption of the MP in the visible light region was enhanced, suggesting some interactions between the BAT-iDP and Lys. The BAT-iDP has one absorption band centered at 299 nm in the ultraviolet region, which could be attributed to the π–π* transition. [42] Lys also has one absorption band centered at 301 nm, which could also be ascribed to the π–π* transition. For MP, its absorption band is centered at 311 nm, which is red-shifted 12 nm or 10 nm compared with the absorption bands of BAT-iDP or Lys. This broadened absorption band of MP could be assigned to the transition of n–π* in the Schiff-base moiety. [43] In general, as the conjugation effect of the molecular system increases, the energy of the π−π* transition decreases, and the absorption peak will be red-shifted. [44] In comparison, without the electron-withdrawing group (−Cl), the BAT-iDP does not show any absorption peak centered at 311 nm in the UV region, and the absorption at 311 nm of BLP is much lower than that of MP. Therefore, these data suggest that −Cl contributed to intensifying the chromophoric property of MP.

Green Chemistry

ARTICLE

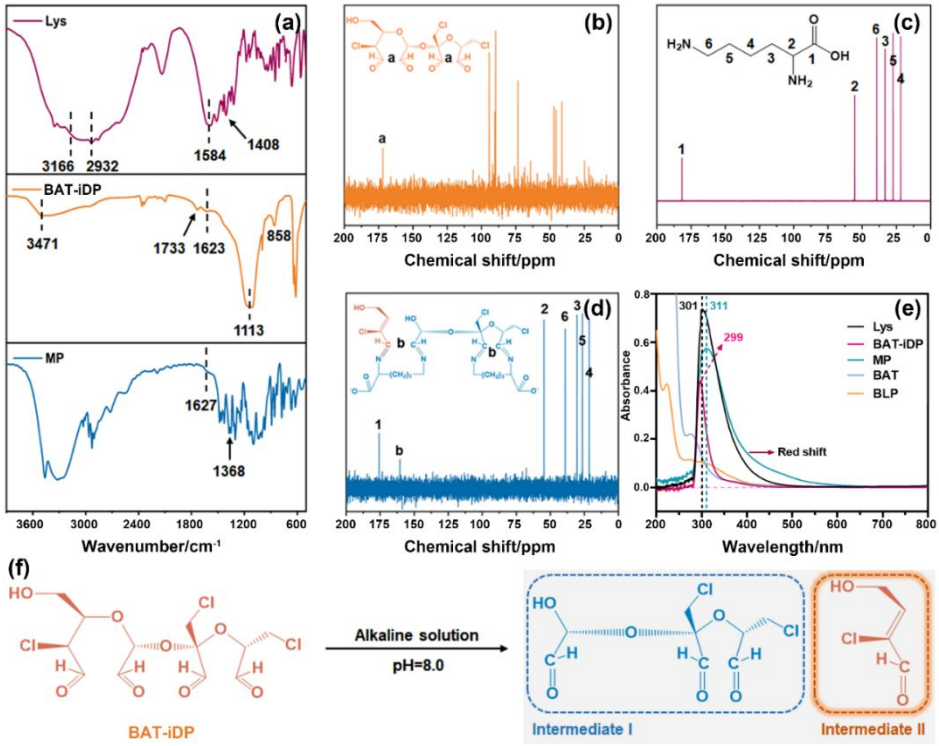

Fig. 5. FTIR (a), NMR (b, c, d), and UV-vis (e) spectra of BAT-iDP, Lys and the reaction product between BAT-iDP and Lys (MP); the structural transition of BAT-iDP under alkaline conditions (f).

BAT-iDP and Lys were mixed uniformly in an aqueous medium. After that, the pH of the reaction liquor was gradually raised to 8.0 and left at 40 °C for 4 h. As shown in Fig. 5f, during this alkalization procedure, the BAT-iDP underwent *β*- alkoxycarbonyl elimination at C5 of the original D-glucose unit, and its structure was accordingly cleaved, [45] forming intermediate I and intermediate II. In light of the above results and considering the structure of BAT-iDP, it can be speculated that the product formed after the reaction between the BAT-iDP and Lys has a conjugated structure containing a Schiff-base and auxochrome species (−Cl). In detail, the as-formed intermediate II containing auxochrome (-Cl) and one −CH=O could react with one of the $-NH_2$ of Lys to form a Schiff-base structure. Meanwhile, the intermediate I containing three −CH=O could synchronously react with the residual $-NH_2$ of Lys that had reacted with intermediate II, and two −CH=O on another molecule of Lys (Fig. 5d).

Based on the above modelling reactions between the BAT-iDP and Lys, Fig. 6 describes the possible tanning and in-situ dyeing mechanism of BAT-iDP. On the one hand, the −CH=O from intermediate I would react with the $-NH_2$ from different CFs in leather to form stable multipoint Schiff-base covalent cross-linkages, which are responsible for the tanning effect. As a result, the BAT-iDP tanned leather has favorable hydrothermal stability and fiber dispersion. On the other hand, the single −CH=O from intermediate II could only react with one $-NH_2$ from CFs, thus forming a single point of Schiff-base covalent crosslinking. In addition to these developments, in this 'One bird two stones' strategy, the formation of a conjugated structure containing Schiff-base and an auxochrome of −Cl also takes place, which endows the tanned leather with a specific brown color (Fig. 4a). Fig. 6(b-d) illustrates the major ways in which the chromophores were combined in the crust leather. As aforementioned, BAT-iDP can combine with CFs via forming Schiff-base covalent crosslinks, and the chromophore is linked to the Schiff-base structure (Fig. 6a). Thus, the colorant derived from the BAT-iDP has relatively higher stability in the leather matrix than those obtained in a two-step process (tanning followed by dyeing). For example, SD is a kind of anionic small molecule dye containing a sulfonate group, which is adsorbed on the CFs mainly via the weak electrostatic attractions (Fig. 6c). CD is also a kind of anionic dye while it has larger molecules than SD and contains more oxygen-containing groups. Thus, the CD can form hydrogen bonds with CFs and deposit among the CFs via the aggregation of dyes through acid-fixation in the later stage of the dyeing process (Fig. 6d), possibly showing higher binding strength than SD in the leather matrix. Given the advantage of bonding fastness to leather, our novel BAT-iDP shows better coloring than SD and CD as tanning and dyeing occur almost simultaneously.

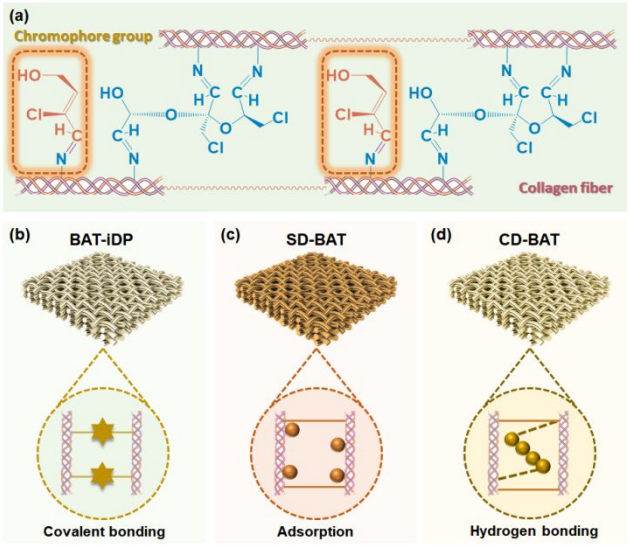

Fig. 6. The proposed tanning and in-situ dyeing mechanism (a), and the major ways in which the chromophores were combined in the crust leather (b: BAT-iDP; c: SD; d: CD).

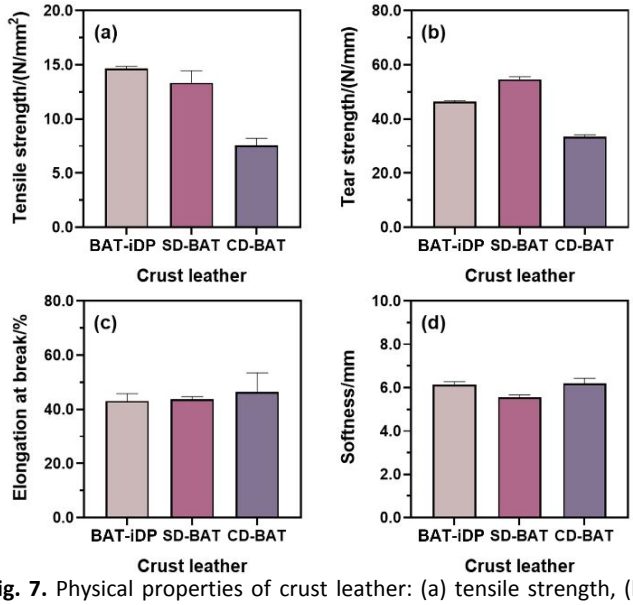

Fig. 7. Physical properties of crust leather: (a) tensile strength, (b) tear strength, (c) elongation at break (c), and (d) softness.

Physical properties of leather

The physical properties of different crust leathers were further measured to evaluate the commercial acceptability. As illustrated in Fig. 7a, the BAT-iDP crust leather has a slightly higher tensile strength than SD-BAT crust leather, which is superior to that of CD-BAT crust leather. This tensile strength (14.7 N/mm^2) is even higher than that of a traditional Cr-tanned crust leather prepared using a similar post-tanning process. [46] As shown in Fig. 7b, the BAT-iDP crust leather has a much higher tear strength than CD-BAT crust leather, despite this being slightly lower than that of SD-BAT crust leather. This tear strength (46.3 N/mm) is comparable to conventional chrome-tanned crust leather prepared using a similar post-tanning process. [46] Owing to the similar crosslinking type of CFs in the leather matrix, these three kinds of crust leather have a comparable elongation at break (Fig. 7c). Fig. 7d illustrates that the BAT-iDP crust leather has a similar softness to that of SD-BAT and CD-BAT crust leathers due to the similar flexible molecular chains in BAT-iDP and BAT. Besides, they also present a comparable CFs lubrication degree as the same amount of tanning agent was used in both cases. In light of the excellent tanning effect, combined with the in-situ dyeing performance of the BAT-iDP, reflected on a tanned leather meeting commercial standards for most kinds of leathery products, our 'Two Birds with One Stone' strategy can simultaneously decrease pollution and potential health hazards derived from the use of Cr and synthetic dyes in the leather industry. However, considering the limited variety of colors at present, in the future, it will be necessary to further develop organic tanning agents with in-situ dyeing properties that can endow leather with more diverse color characteristics, e.g., three-primary colors, to promote their industrial applications. Additionally, QM or molecular mechanics calculations could also be used to gain more insights into this novel and almost unexplored technology.

Conclusions

This work addresses a pioneering 'Two Birds with One Stone' strategy for processing chrome-free and dye-free colored leather using a biomass-derived aldehyde tanning agent with in-situ dyeing properties (BAT-iDP). This novel tanning agent was prepared from sucralose as it contains a special electron-withdrawing group (−Cl) used as the path-breaker. The colorless and transparent aqueous solution containing the BAT-iDP exhibited a well-pleasing tanning effect in terms of high thermal stability and collagen fiber (CF) dispersion of tanned leather. The simulated reaction analysis revealed that the in-situ formation of conjugated structures containing the Schiff-bases and auxochromes (−Cl) accompanied by the crosslinking reaction during the tanning process endowed the BAT-iDP tanned leather with a specific and well-accepted brown color. The stable crosslinking-coloring structures were responsible for the excellent coloring performance of the BAT-iDP crust leather. Besides, the crust leather also had available mechanical strengths for commercial use, suggesting its favorable potential for the production of leather products. As a result, this 'Two Birds with One Stone' strategy exemplified by our pioneering BAT-iDP is a more environmentally friendly option for leather production, which can simultaneously substitute hazardous Cr-based tanning agents and toxic dyes. Besides, it provides inspirational new insights into leather tanning and dyeing, creating an avenue toward achieving a greener and carbon-neutral leather industry development.

Experimental

Materials

Sigma-Aldrich provided analytical-grade sucralose and sodium periodate. A conventional BAT was obtained via a previously reported preparation method. [46] Sinopharm Chemical Reagent Co., Ltd. provided biochemical-grade L-lysine (Lys). The commercial small-molecular dye SD: Orange G, C.I. 16230 was provided by Shanghai Aladdin Biochemical Technology Co., Ltd, while the

commercial leather brown dye (CD) was purchased from Everlight Chemical. Hebei Dongming Leather Co., Ltd provided pickled cattle hide. Other leather chemicals for wet-finishing were industrial grade and purchased from Sichuan Tingjiang New Material, Inc. and Sichuan Dowell Science and Technology Inc.

Preparation of BAT-iDP

20.0 g sucralose was dissolved in deionized water, followed by the slow addition of 21.5 g sodium periodate under continuously stirring at 10 °C. After reaction in the dark for 12 h under a mild stirring, the product was filtered by vacuum filtration, and the filtrate was finally lyophilized to obtain the solid BAT-iDP.

Tanning and post-tanning trials

Pickled cattle hide was treated with water containing 4% BAT-iDP (based on the twice weight of the pickled cattle hide) at 25°C for 4 h, adjusting the liquor with a 4% sodium bicarbonate solution until pH 8.0. After that, the tanning temperature was raised to 40 °C and the process was kept for another 4 h. Finally, the BAT-iDP tanned leather was prepared. Besides, the BAT was synthesized via the previously reported method, [24] and employed for the tanning of pickled cattle hide to prepare BAT tanned leather with white color under the same tanning conditions. The dyeing of the BAT tanned leather using SD and CD was conducted for comparison. The detailed post-tanning trial conditions for the tanned leather are presented in Table S1 in the Supplementary Material.

Reactions between the BAT-iDP and Lys

10 mL of BAT-iDP solution (20 g/L) and 10 mL of Lys solution (20 g/L) were intimately mixed, and then sodium bicarbonate was introduced to adjust the solution pH to 8.0. Afterward, the solution was heated to 40 °C and kept for 4 h. Finally, the resultant solution was lyophilized to obtain the dry model product (MP) for further structural characterization. The BAT-iDP, Lys and MP solutions were diluted by an appropriate multiple for UV-vis spectroscopic analysis (UV-1200, Mapada, China). The BAT was then used to react with Lys under the same conditions, and the UV-vis spectra of BAT and the reaction products were recorded at the same dilution ratio as for BAT-iDP and MP for comparison.

FTIR and NMR spectroscopies

FTIR spectra for sucralose, BAT-iDP and the simulated reaction product between BAT-iDP and Lys were carried out on a TENSOR 27 spectrometer (Brook, Germany) at the wavenumber range from 400 cm^{-1} to 4000 cm^{-1} with a resolution of 4.0 cm^{-1}. All samples were made into tablets with a proportion of KBr. The NMR spectra of the aforementioned samples were determined using an NMR spectrometer (Avance III 400 MHz, Bruker, Switzerland). The sample was dissolved in D_2O, and its concentrations for ^1H NMR and ^{13}C NMR tests were around 20 g/L and 80 g/L, respectively.

Physical properties and dyeing performance

Leather samples were lyophilized first, and then their cross-sections were observed by a scanning electron microscope (Phenom Pro X, Phenom Scientific, Netherlands) with an accelerating voltage of 15 kV. The shrinkage temperature (Ts) is the most commonly used index to characterize the hydrothermal stability of leather. [47] The Ts of pickled hide and tanned leather were determined using a leather Ts tester (MSW-YD4, Sunshine Electronic Research Institute, China). The thermal stability of the lyophilized leather sample was further measured using a TG-DSC thermal analyzer (STA-8000, PerkinElmer, USA).

The coloring performance of crust leathers from different tanning and dyeing processes was assessed using the previously reported method [46]. At first, 'L', 'a', 'b' chromatic values from eight random points on crust leathers were measured by a colorimeter (Color reader CR-13, Konica Minolt, Japan). The ΔE value (total color difference) was calculated according to Eq. 1. For this measurement, one given sampling point was used as the standard, and the ΔE of other seven points on crust leather was also determined and used to calculate dispersion. For this, the STDEV (standard deviation) of seven ΔE values was calculated to estimate the dyeing uniformity. Generally, a lower STDEV value of ΔE means a higher dyeing uniformity.

$$\Delta E = \sqrt{(\Delta L)^2 + (\Delta a)^2 + (\Delta b)^2} \quad (1)$$

Besides, the color fastness to dry-wet rubbing of the resultant crust leather was evaluated using the method reported by Li et al. [48] Furthermore, 10 g of the crust leather was sampled and cut into small pieces (0.3 cm × 0.3 cm). Subsequently, these samples were added into a flask containing 100 mL of ultrapure water (UPW) and shaken at 40 °C for 24 h. After vacuum filtration, the visible spectra of the extract liquors were determined in a UV-1200 ultra-violet and visible spectrophotometer (Mapada, China).

Before testing the physical properties, the naturally dried crust leather samples were further air-conditioned for 48 h at 20 °C and 65% RH. After that, the softness was measured via a GT-303 standard leather softness tester (Gotech Testing Machines Inc., China), [49] and the mechanical strengths, including tensile strength, tear strength and elongation at break, were further determined according to the standard methods [50] using a tensile tester (AI-7000SN, Gotech, China).

Author Contributions

Wei Ding: Conceptualization, Writing - Original Draft, Investigation, Funding acquisition; **Javier Remón:** Investigation, Review & Editing; **Zhicheng Jiang:** Investigation, Review & Editing.

Conflicts of interest

There are no conflicts to declare.

Acknowledgments

The authors thank the financial support from the National Natural Science Foundation of China (22108297) and the National Key Research and Development Program (2020YFE0203800). Javier Remón thanks the Spanish Ministry of Science, Innovation and Universities for his Juan de la Cierva (JdC) fellowship (IJC2018-037110-I).

Notes and references

1 Z. Jiang, W. Ding, S. Xu, J. Remón, B. Shi, C. Hu and J. H. Clark, *Green Chem.*, 2020, **22**, 316–321.
2 Z. Jiang, S. Xu, W. Ding, M. Gao, J. Fan, C. Hu, B. Shi and J. H. Clark, *Green Chem.* , 2021, **23**, 4044–4050.
3 T. Qiang, X. Gao, J. Ren, X. Chen and X. Wang, *ACS Sustainable Chem. Eng.*, 2016, **4**, 701–707.
4 Y. Yu, Y. Lin, Y. Zeng, Y. Wang, W. Zhang, J. Zhou and B. Shi, *ACS Sustainable Chem. Eng.*, 2021, **9**, 6720-6731.
5 K. Li, H. Chen, Y. Wang, Z. Shan, J. Yang and P. Brutto, *J. Cleaner Prod.*, 2009, **17**, 1603–1606.
6 Y. Wang, W. Huang, H. Zhang, L. Tian, J. Zhou and B. Shi, *J. Am. Leather Chem. Assoc.,* 2017, **112**, 224–231.
7 M. Kumar, N. Fathima, R. Aravindhan, J. Rao and B. Nair, *J. Am. Leather Chem. Assoc.,* 2009, **104**, 113–119.
8 B. Shi, J. Li, Y. N. Wang, X. Liao, W. Zhang, Q. He and M. Cao, in *Taipei: 9th AICLST Congress*, 2012, pp. 1–18.
9 X. Liu, W. Wang, X. Wang, S. Sun and C. Wei, *J. Cleaner Prod.*, 2021, **319**, 128658.
10 A. D. Covington, *Tanning chemistry: the science of leather*, Royal Society of Chemistry, Cambridge, 2009.
11 J. Shi, C. Wang, L. Hu, Y. Xiao and W. Lin, *ACS Sustainable Chem. Eng.*, 2018, **7**, 1195–1201.
12 X. Wang, S. Sun, X. Zhu, P. Guo, X. Liu, C. Liu and M. Lei, *J. Leather Sci. Eng.*, 2021, **3**, 1–9.
13 S. Xu, X. Niu, Z. Hou, C. Gao, J. Lu, Y. Pang, M. Fang, Y. Lu, Y. Chen and K. S. Joshy, *J. Hazard. Mater.,* 2020, **383**, 121142.
14 W. Ding, S. Guo, H. Liu, X. Pang and Z. Ding, *Mater. Today Chem.*, 2021, **21**, 100508.
15 J. Rovira and J. L. Domingo, *Environ. Res*, 2019, **168**, 62–69.
16 S. Bordingnon, M. Gutterres, S. K. Velho, W. F. Fuck, A. V Schor, M. Cooper and L. Bresolin, *J. Asocia. Quím. Espanõl. Ind. Cuer*, 2012, **63**, 93–99.
17 X. Chen, K. Ding and L. Jun, *Dyes and Pigments*, 2015, **123**, 404–412.
18 B. Zhang, L. Xu and K. Ding, *J. Am. Leather Chem. Assoc.,* 2011, **106**, 121–126.
19 B. Zhang, L. Xu and K. Ding, *J. Am. Leather Chem. Assoc.,* 2011, **106**, 303–308.
20 K. Ding, M. M. Taylor and E. M. Brown, *J. Am. Leather Chem. Assoc.,* 2006, **101**, 362–367.
21 T. Qiang, L. Chen, Q. Zhang and X. Liu, *J. Cleaner Prod.*, 2018, **197**, 1117–1123.
22 W. Ding, X. Pang, Z. Ding, D. C. W. Tsang, Z. Jiang and B. Shi, *J. Hazard. Mater.,* 2020, **396**, Article 122771.
23 W. Ding and Y. Wu, *Carbohydr. Polym.,* 2020, **248**, 116801.
24 W. Ding, J. Zhou, Y. Zeng, Y. nan Wang and B. Shi, *Carbohydr. Polym.,* 2017, **157**, 1650–1656.
25 W. Ding, Y. Wang, J. Zhou and B. Shi, *Carbohydr. Polym.,* 2018, **201**, 549–556.
26 W. Ding, Y. Wang, J. Zhou, H. Liu, X. Pang and B. Shi, *J. Leather Sci. Eng.*, 2021, **3**, 5.
27 R. L. Whistler, P. K. Chang and G. N. Richards, *J. Am. Chem. Soc.*, 1959, **81**, 3133–3136.
28 R. L. Whistler, P. K. Chang and G. N. Richards, *J. Am. Chem. Soc.*, 1959, **81**, 4058–4060.
29 V. G. Malshet and L. Al Tappel, *Lipids*, 1973, **8**, 194.
30 F. S. Santos, T. M. H. Costa, V. Stefani, P. F. B. Goncalves, R. R. Descalzo, E. V Benvenutti and F. S. Rodembusch, *The J. Phys. Chem. A*, 2011, **115**, 13390–13398.
31 M. V. L. Motta, E. V. R. de Castro, E. J. B. Muri, M. L. Costalonga, B. V. Loureiro and P. R. Filgueiras, *Int. J. Biol. Macromol.,* 2019, **121**, 23–28.
32 L. Liang, T. Hou, Q. Ouyang, L. Xie, S. Zhong, P. Li, S. Li and C. Li, *Compos. Part B-Eng.*, 2020, **188**, 107877.
33 H. Yang and T. G. M. van de Ven, *Cellulose*, 2016, **23**, 1791–1801.
34 N. S. Cohen, M. Odlyha and G. M. Foster, *Thermochim. Acta*, 2000, **365**, 111–117.
35 L. Yu, X. Qiang, L. Cui, B. Chen, X. Wang and X. Wu, *J. Cleaner Prod.*, 2020, **270**, 122351.
36 J. Liu, L. Luo, Y. Hu, F. Wang, X. Zheng and K. Tang, *J. Leather Sci. Eng.*, 2019, **1**, 9.
37 S. Z. Pu, Y. N. Wang, Q. He, X. P. Liao, W. H. Zhang and B. Shi, *Int. J. Quantum Chem.*, 2012, **112**, 2832–2839.
38 S. Kumari and G. S. Chauhan, *ACS Appl. Mater. Inter.*, 2014, **6**, 5908–5917.
39 L. Zhang, P. Yan, Y. Li, X. He, Y. Dai and Z. Tan, *Ind. Crops Prod.,* 2020, **145**, 112126.
40 S. M. A. S. Keshk, A. M. Ramadan and S. Bondock, *Carbohydr. Polym.,* 2015, **127**, 246–251.
41 N. Srisawang, S. Nobsathian, S. Wirasate and C. Chitichotpanya, *Macromol. Res.*, 2019, **27**, 1193–1199.
42 V. K. Gupta, A. K. Singh, M. R. Ganjali, P. Norouzi, F. Faridbod and N. Mergu, *Sensor. Actuat. B-Chem.*, 2013, **182**, 642–651.
43 S. Arunachalam, N. P. Priya, C. Jayabalakrishnan and V. Chinnusamy, *Int. J. Appl. Bio. Pharm. Tech.*, 2011, **2**, 370–377.
44 X. Mu, K. Cai, W. Wei, Y. Li, Z. Wang and J. Wang, *The J. Phys. Chem. C*, 2018, **122**, 7831–7837.
45 S. Veelaert, D. De Wit, K. F. Gotlieb and R. Verhé, *Carbohydr. Polym.,* 1997, **33**, 153–162.
46 W. Ding, Y. Yi, Y. Wang, J. Zhou and B. Shi, *Carbohydr. Polym.,* 2019, **224**, 115169.
47 Y. Zhou, J. Ma, D. Gao, W. Li, J. Shi and H. Ren, *J. Cleaner Prod.*, 2018, **201**, 668–677.
48 J. Li, Y. Wang and B. Shi, *Leather Sci. Eng.*, 2018, **28**, 41–47.
49 IUP 36, *J. Soc. Leather Technol. Chem.*, 2000, **84**, 377–379.
50 IUP 6, *J. Soc. Leather Technol. Chem.*, 2000, **84**, 317–321.